ANTIMICROBIAL AGENTS AND CHEMOTHERAPY, Sept. 1992, p. 1810–1816
0066-4804/92/091810-07$02.00/0

Vol. 36, No. 9

Prediction of Human Pharmacokinetics of Panipenem-Betamipron, a New Carbapenem, from Animal Data

ATSUSHI KURIHARA,[1]* HIDEO NAGANUMA,[1] MASAFUMI HISAOKA,[1] HIROSHI TOKIWA,[2] AND YUKINORI KAWAHARA[2]

Product Development Laboratories[1] and Analytical and Metabolic Research Laboratories,[2] Sankyo Co., Ltd., Hiromachi, Shinagawa-ku, Tokyo 140, Japan

Received 12 November 1991/Accepted 10 June 1992

The pharmacokinetic behavior of panipenem (PAPM)-betamipron (BP), a new carbapenem, in humans was successfully predicted from data collected from six animal species. PAPM and BP were biphasically eliminated from plasma after intravenous (i.v.) administration of PAPM-BP to mice, guinea pigs, rats, rabbits, monkeys, and dogs. Elimination rates of PAPM and BP were correlated with animal size: the larger the animal was, the slower the elimination was. As for PAPM and BP, log-log plots of total plasma clearance (CL_{tot}) versus body weight and log-log plots of distribution volume at steady state (V_{SS}) versus body weight for six animal species were linear, with high correlation coefficients. These allometric equations were extrapolated to predict CL_{tot} and V_{SS} for PAPM and BP in humans. In addition, concentration in plasma-time profiles for humans were predicted by using two-exponent equations fitted to the complex Dedrick plot of animal data. Predicted values for CL_{tot} and V_{SS} for PAPM and BP in humans agreed well with observed values in humans given 750/750 mg of PAPM-BP as an i.v. drip infusion for 30 min. Predicted concentration in plasma-time profiles for humans approximated observed profiles. Thus, the pharmacokinetics of PAPM-BP extrapolated well from animal species to humans when allometric equations and the complex Dedrick plot were used.

Panipenem (PAPM)-betamipron (BP) is a combination of a newly developed carbapenem antibiotic (PAPM) and a renal anion transport inhibitor (BP) in a ratio of 1:1 (wt/wt) (Fig. 1). PAPM has a broad antibacterial spectrum against gram-positive and gram-negative organisms and is stable against hydrolysis by various types of beta-lactamase (7). BP decreases nephrotoxicity caused by very high doses of PAPM in rabbits via inhibition of PAPM accumulation in the renal cortex (15).

In developing new drugs, it is very important to predict the drug concentration in plasma in humans by using animal scale-up, because efficacy or toxicity of the drug is generally correlated with its concentration in plasma. Even though the final determinant of efficacy or toxicity is not the concentration in plasma but a certain concentration in tissue, plasma kinetics provides basic information about distribution of the drug in tissue.

Several reports dealing with animal scale-up by allometric scaling have recently been published. For example, animal scale-ups of aztreonam (19), nimustine (ACNU) (12), and acivicin (11) have been successfully performed.

The present study was designed to examine the disposition and pharmacokinetics of PAPM-BP in six animal species and to predict pharmacokinetics in humans from animal data. For prediction, allometric equations of body weight (BW) and of pharmacokinetic parameters and the complex Dedrick plot (2) were used. In addition, the predicted values were compared with those observed in clinical trials.

MATERIALS AND METHODS

Chemicals. PAPM [(5*R*,6*S*)-3[(*S*)-1-(acetimidoylpyrrolidin-3-yl)thio]-6-[(*R*)-1-hydroxyethyl]-7-oxo-1-azabicyclo[3,2,0]hept-2-ene-carboxylic acid] and BP (*N*-benzoyl-beta-alanine) were synthesized at Sankyo Co., Ltd. All other reagents and solvents were commercial products of analytical and high-performance liquid chromatography (HPLC) grade.

Animal experiments. Animal pharmacokinetic studies were conducted in male ddY mice (18 to 22 g), male Hartley guinea pigs (280 to 320 g), male Wister-Imamichi rats (290 to 310 g), male Japanese White rabbits (2.5 to 3.5 kg), female cynomolgus monkeys (3 to 4 kg), and male beagle dogs (10 kg). PAPM-BP was dissolved in sterile saline just before being administered to experimental animals at doses of 10/10 to 50/50 mg/kg of body weight. Groups of mice were given PAPM-BP as an intravenous (i.v.) bolus in the tail vein and were bled by decapitation at appropriate times. Studies in other animal species were performed with i.v. bolus administration followed by serial blood sampling. With guinea pigs and rats, femoral artery catheters were utilized for blood sampling. Heparinized blood from each animal species was centrifuged at 2,500 × *g* for 10 min to obtain plasma samples. In studies of urinary excretion, PAPM-BP was administered i.v. at a dose of 10/10 mg/kg to all animals except dogs. Dogs were administered the drug at a dose of 50/50 mg/kg for evaluation of the dosage for clinical trials. Urine samples were collected for 24 h from mice, guinea pigs, and rats; for 3 h from rabbits and dogs; and for 5 h from monkeys. Obtained plasma and urine samples were added to equal volumes of 1 M MOPS [3-(*N*-morpholino)propanesulfonic acid; pH 7.0] for the stabilization of PAPM, and they were kept at −40°C until assay.

Clinical trials. PAPM-BP (750/750 mg) was dissolved in 100 ml of sterile saline and administered to five healthy male human volunteers (age, 21 ± 2 years; BW, 61 ± 5 kg; height, 167 ± 5 cm [means ± standard deviations]). Serial blood and urine samples were collected for 24 h and were treated as described above for the assay.

Analytical method. The concentrations of PAPM in plasma and urine were determined by the HPLC assay or microbiological assay developed by Hisaoka et al. (5, 6). The concentrations of BP in plasma and urine were determined

* Corresponding author.

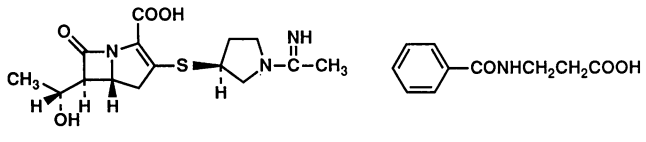

PAPM BP

FIG. 1. Chemical structures of PAPM and BP.

by the HPLC method described by Hisaoka et al. (6). The limits of detection of PAPM were 0.3 μg/ml for plasma and 1.0 μg/ml for urine in HPLC and 0.02 μg/ml for both plasma and urine in the microbiological assay; those of BP were 0.2 μg/ml for plasma and 0.5 μg/ml for urine. Linearities of the assay were obtained within the concentration range of 0 to 50 μg/ml for both PAPM and BP. In addition, coefficients of variation over the linear concentration range were less than 5% for PAPM and BP both within and between days. Previous studies have indicated that no active metabolite of PAPM is detected in plasma or urine after administration of PAPM-BP to experimental animals and humans and that there is a good correlation between HPLC assay and microbiological assay (5).

Pharmacokinetic analysis. Pharmacokinetic parameters for PAPM and BP in animal species were calculated from the concentration in plasma-time profiles by using noncompartmental analysis (20). The following equations, CL_{tot} = dose/AUC, V_{SS} = CL_{tot} × MRT, and CL_R = CL_{tot} × f(urine), where CL_{tot} is the total plasma clearance, AUC is the area under the concentration in plasma-time curve, V_{SS} is the volume of distribution at steady state, MRT is the mean residence time in the body, CL_R is the renal clearance, and f(urine) is the fraction of a dose excreted in urine as an unchanged compound, were used. Half-life was calculated from the terminal slope in a semilog plot of the concentration in plasma versus time by generalized least-squares regression.

Prediction of human pharmacokinetics. The CL_{tot}, V_{SS}, and BW data for PAPM and BP in experimental animals were log transformed and fitted to the following equations by generalized least-squares methods.

$$CL_{tot} = a \times BW^{x} \quad (1)$$

$$V_{SS} = b \times BW^{y} \quad (2)$$

These regression lines were then extrapolated to a human BW of 60 kg to obtain estimates for CL_{tot} and V_{SS} for PAPM and BP in humans. Concentration in plasma-time profiles for PAPM and BP in humans (30-min drip infusion of 750/750 mg of PAPM-BP) were simulated by using the complex Dedrick plot (2) as follows. Transformed time (T*) and concentration in plasma (Cp*) for humans were defined as follows: T^* = real time × $[(BW_{human})^{y-x}/(BW_{animal})^{y-x}]$ and Cp^* = $Cp_{animal} \times [(BW_{human})^{1-y}/(BW_{animal})^{1-y}]$, where real time is the chronological sampling time in animal experiments, x and y are the respective power components in equations 1 and 2, and Cp_{animal} is the normalized concentration in plasma of PAPM and BP for a 750/750-mg/60-kg dose based on data from the 25/25-mg/kg dose in experimental animals. Each value of Cp* for all experimental animals was plotted against the corresponding T^* (complex Dedrick plot). Then, all points in the complex Dedrick plot were fitted to the two-exponent equations described below by using a nonlinear least-squares method with program MULTI (21).

$$Cp^* = (A \times e^{-\alpha T^*}) + (B \times e^{-\beta T^*}) \quad (3)$$

From the hybrid constants A, B, α, and β in equation 3, predicted concentration in plasma-time profiles for PAPM and BP during and after a 30-min drip infusion of PAPM-BP (750/750 mg per body) were calculated with the following equations.

When $t \leqq 0.5$ h:

$$Cp = A[(1 - e^{-\alpha t})/(\alpha \times 0.5)] + B[(1 - e^{-\beta t})/(\beta \times 0.5)] \quad (4)$$

When $t \geqq 0.5$ h:

$$Cp = \{A[(1 - e^{-\alpha \times 0.5})/(\alpha \times 0.5)] \times e^{-\alpha \times (t - 0.5)}\} + \{B[(1 - e^{-\beta \times 0.5})/(\beta \times 0.5)] \times e^{-\beta \times (t - 0.5)}\} \quad (5)$$

Serum protein binding. Serum protein binding of PAPM and BP was determined by ultrafiltration with a micropartition system (Centrifree; Amicon Division, W. R. Grace & Co., Beverly, Conn.). In preliminary experiments, no adsorption of PAPM and BP to the Centrifree system was observed. PAPM and BP were added to fresh serum obtained from animal species and humans to produce final concentrations of 10, 50, and 100 μg/ml for PAPM and 10, 20, and 40 μg/ml for BP. Then, plasma was incubated at 0°C

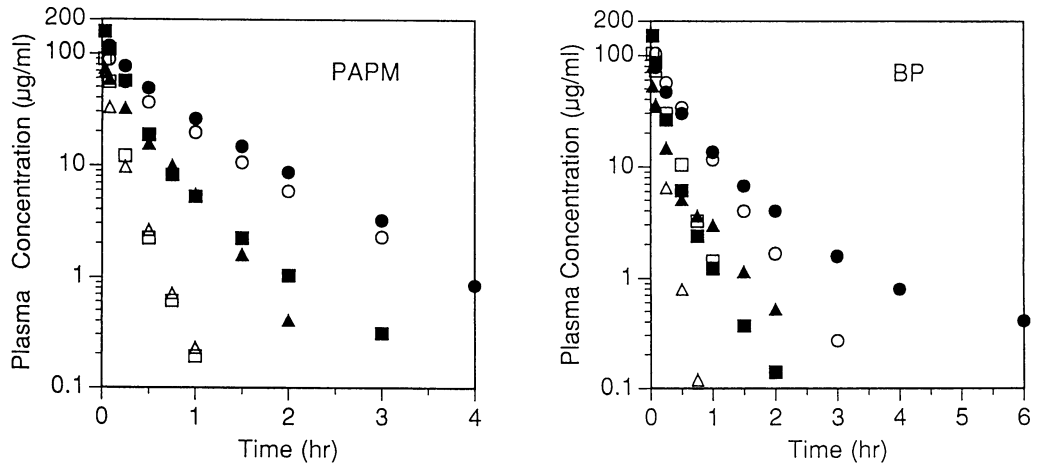

FIG. 2. Concentrations of PAPM and BP in plasma after i.v. administration of PAPM-BP (25/25 mg/kg) to mice (△), guinea pigs (▲), rats (□), rabbits (■), monkeys (○), and dogs (●). Each value represents the mean for three to six animals.

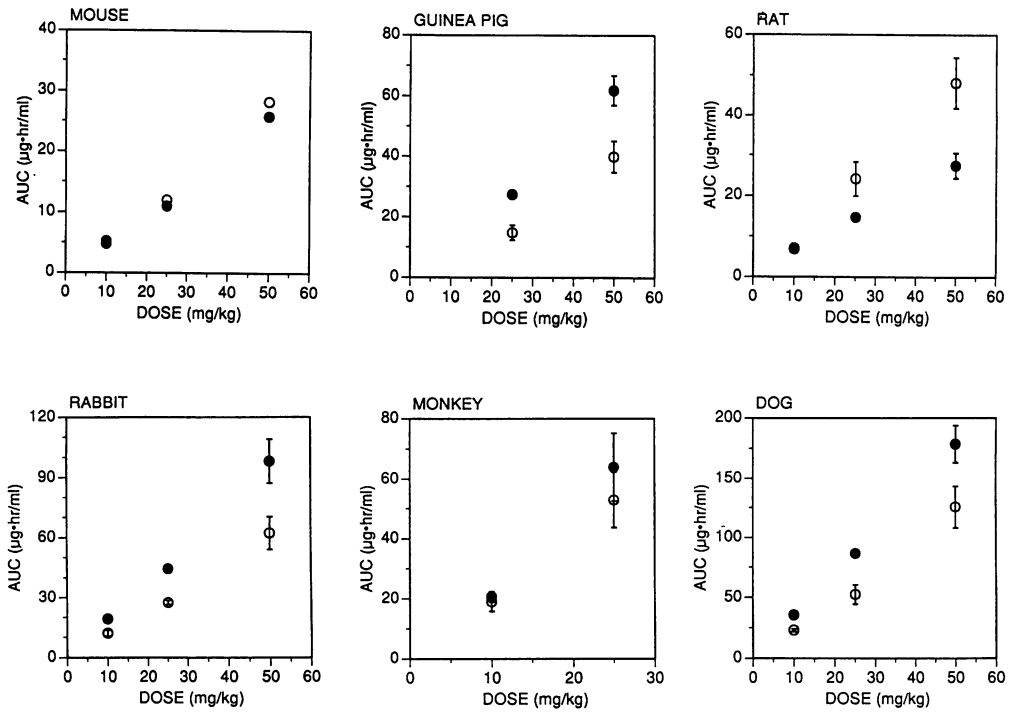

FIG. 3. Relationship between dose and AUC for PAPM (●) and BP (○) after i.v. administration of PAPM-BP to experimental animals. Each point and vertical bar represents the mean ± standard error of the mean for three to six animals. AUCs for mice were calculated from the mean concentration in plasma-time profiles.

for 30 min. An aliquot was loaded onto the Centrifree system and centrifuged at 500 × g for 15 min at 0°C. The fraction of unbound drug in serum (f_U) was calculated as the ratio of the concentration in ultrafiltrates to the concentration in serum.

RESULTS

Pharmacokinetics of PAPM-BP in experimental animals. Mean concentration in plasma-time profiles for PAPM and BP after i.v. bolus administration of 25/25 mg of PAPM-BP per kg to mice, guinea pigs, rats, rabbits, monkeys, and dogs are shown in Fig. 2. In every animal species, PAPM and BP were biphasically eliminated from plasma. Elimination rates of PAPM and BP were correlated with animal size. The larger the animal was, the slower the elimination was. Figure 3 shows the relationship between dose and AUC after i.v. administration of various doses of PAPM-BP in six animal species. In each animal species, there existed a linear correlation between administered dose and AUC both for PAPM and for BP, suggesting linear pharmacokinetics. Pharmacokinetic parameters of PAPM and BP after i.v. administration of PAPM-BP (25/25 mg/kg) to experimental animals were calculated from the mean concentration in plasma-time profiles and listed in Table 1. The dose fractions

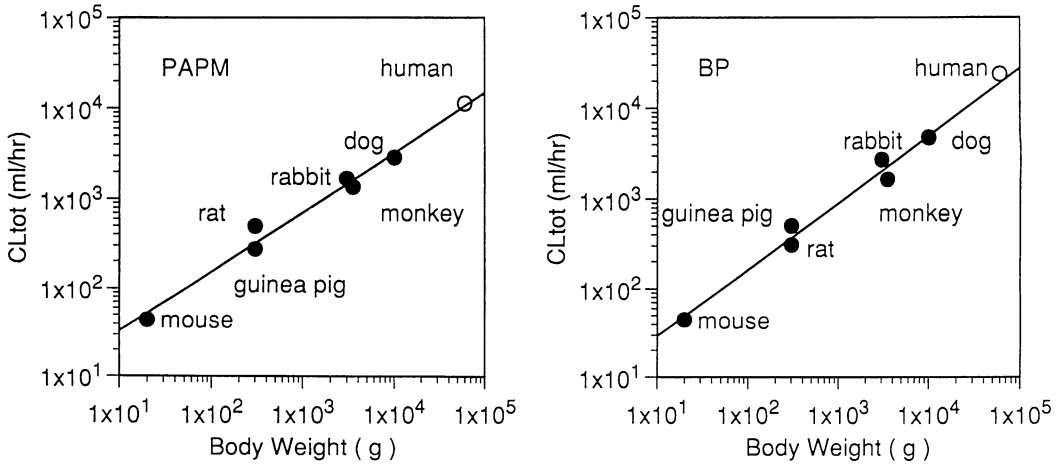

FIG. 4. Allometric plots of CL_{tot} for PAPM and BP as a function of animal BW. Each point represents a value listed in Table 1. The open circle denotes the value observed in humans. Regression lines were determined by least-squares analysis of the data, excluding human data.

TABLE 1. Pharmacokinetic parameters of PAPM and BP after i.v. administration of PAPM/BP (25/25 mg/kg) to experimental animals[a]

Species	BW (g)	CL_{tot} (ml/h)	V_{SS} (ml)	Half-life (h)	f(urine)[b]	CL_R (ml/h)	f_U[c]
PAPM							
Mouse	20	44.4	5.78	0.14	0.404	18	ND
Guinea pig	300	275	102	0.29	0.065	18	ND
Rat	300	498	56.7	0.13	0.394	196	0.955
Rabbit	3,000	1,690	540	0.45	0.588	994	0.916
Monkey	3,500	1,370	1,040	0.62	0.303	415	0.933
Dog	10,000	2,910	2,150	0.49	0.302	879	0.953
BP							
Mouse	20	45.4	4.54	0.08	0.902	41	ND
Guinea pig	300	507	203	0.48	0.888	450	ND
Rat	300	309	71.1	0.16	0.674	208	0.144
Rabbit	3,000	2,750	495	0.22	0.895	2,461	0.016
Monkey	3,500	1,660	797	0.35	0.407	676	0.281
Dog	10,000	4,810	4,380	0.67	0.610	2,934	0.590

[a] CL_{tot}, V_{SS}, and half-life were calculated from the mean concentration in plasma-time profiles.
[b] Dose was 50/50 mg/kg for dogs and 10/10 mg/kg for the other animals.
[c] f_U, fraction of unbound drug in serum (in vitro), which represents the mean value of 10 to 100 μg/ml for PAPM and 10 to 40 μg/ml for BP. ND, not determined.

excreted in urine [f(urine)] as unchanged PAPM and BP from separate experiments of i.v. administration of PAPM-BP at doses of 10/10 and 50/50 mg/kg and the f_U in vitro are also shown in Table 1. Values of f(urine) for PAPM in six animal species varied from 0.065 (guinea pig) to 0.588 (rabbit). In contrast, values for BP were fairly high, (0.407 to 0.902) in every animal species. Values of f_U for PAPM in each animal species examined were close to unity (0.916 to 0.955), indicating low serum protein binding for PAPM. Values of f_U for BP varied from 0.016 to 0.590 in the animal species examined.

Prediction of human pharmacokinetics. Allometric relationships between CL_{tot} and BW for PAPM and BP in six animal species are shown in Fig. 4. CL_{tot}s in the mouse, guinea pig, rat, rabbit, monkey, and dog were plotted against BW on log-log coordinates. These plots were linear and were fitted to the following allometric equations with high correlation coefficients (r).

$$\text{PAPM: } CL_{tot}\ (\text{ml/h}) = 7.23 \times \text{BW}\ (\text{g})^{0.663}\ (r = 0.986) \quad (6)$$

$$\text{BP: } CL_{tot}\ (\text{ml/h}) = 5.33 \times \text{BW}\ (\text{g})^{0.743}\ (r = 0.989) \quad (7)$$

Equations 6 and 7 were extrapolated to obtain estimates for a 60-kg human (listed in Table 2). V_{SS}s for PAPM and BP in the mouse, guinea pig, rat, rabbit, monkey, and dog were also plotted against body weight on log-log coordinates (Fig. 5). These plots were linear and fitted to the following allometric equations with high correlation coefficients.

$$\text{PAPM: } V_{SS}\ (\text{ml}) = 0.327 \times \text{BW}\ (\text{g})^{0.956}\ (r = 0.994) \quad (8)$$

$$\text{BP: } V_{SS}\ (\text{ml}) = 0.275 \times \text{BW}\ (\text{g})^{1.008}\ (r = 0.975) \quad (9)$$

Equations 8 and 9 were extrapolated to a human BW of 60 kg to obtain predicted human parameters (listed in Table 2). Thus, in both cases with PAPM and BP, good correlations were found between CL_{tot} and BW and between V_{SS} and BW on log-log coordinates. Therefore, predictions of concentration in plasma-time profiles for PAPM and BP in humans were tried by using the complex Dedrick plot for the data from six animal species (Fig. 6). Data on concentrations in plasma for mouse, guinea pig, rat, rabbit, monkey, and dog in the complex Dedrick plot were dispersed in narrower ranges than in the normal plot, as shown in Fig. 2. Fitted lines of the complex Dedrick plot for PAPM and BP were as follows: for PAPM, $Cp^* = (57.1 \times e^{-3.21T^*}) + (28.1 \times e^{-0.572T^*})$, and for BP, $Cp^* = (300 \times e^{-36.0T^*}) + (48.0 \times e^{-1.42T^*})$. These fitted parameters and equations 4 and 5 were used to calculate concentration in plasma-time profiles for PAPM and BP during and after a 30-min drip infusion of

TABLE 2. Pharmacokinetic parameters of PAPM and BP after 30-min i.v. drip infusion of PAPM-BP (750/750 mg per body) in humans

Drug and parameter	BW (kg)	Cp (μg/ml)		CL_{tot} (liter/h)	V_{SS} (liter)	Half-life (h)	f(urine)	CL_R (liter/h)	f_U[a]
		30 min	2 h						
PAPM									
Observed									
Mean	61	61.39	10.35	11.3	11.1	0.84	0.195	2.3	0.961
SD (n = 5)	5	11.04	2.29	1.3	2.3	0.12	0.080	1.1	0.004
Predicted from animals	60	52.87	10.59	10.6	12.1	1.21			
BP									
Observed									
Mean	61	39.01	3.11	23.9	17.3	0.81	0.979	23.4	0.170
SD (n = 5)	5	7.02	0.58	3.0	4.9	0.21	0.032	3.5	0.002
Predicted from animals	60	51.03	4.08	18.9	18.0	0.49			

[a] Fraction of unbound drug in serum (in vitro), which represents the mean value of 10 to 100 μg/ml for PAPM and 10 to 40 μg/ml for BP.

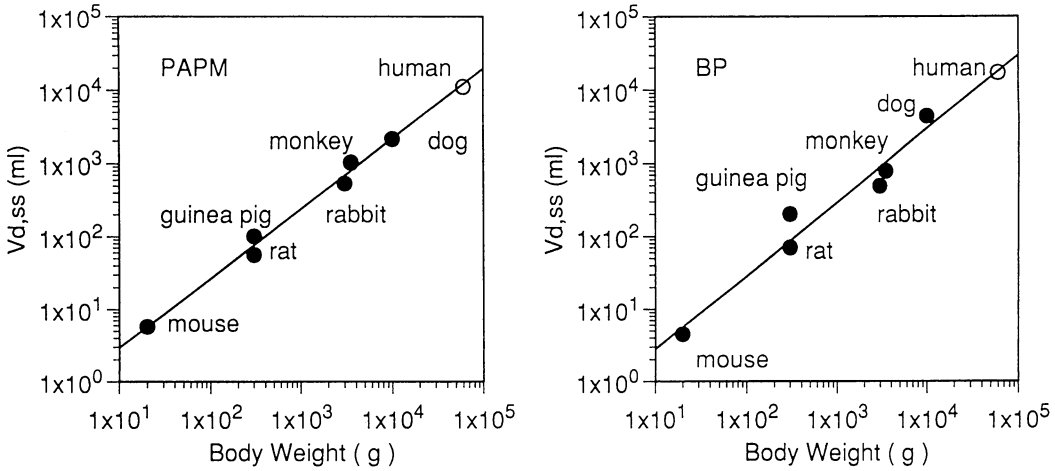

FIG. 5. Allometric plots of V_{SS} (Vd,ss) for PAPM and BP as a function of animal BW. Each point represents a value listed in Table 1. The open circle denotes the value observed in humans. Regression lines were determined by least-squares analysis of the data, excluding human data.

PAPM-BP (750/750 mg per body) in humans, which are presented in Fig. 7 and Table 2. In Fig. 7, observed concentrations in plasma in humans are also shown. Human pharmacokinetic parameters calculated from the observed data for concentrations in plasma are listed in Table 2 with values predicted from animal species. CL_{tot} and V_{SS} for humans are plotted in Fig. 4 and 5, respectively. Predicted values for CL_{tot} in humans (PAPM, 10.6 liter/h; BP, 18.9 liter/h) agreed well with the observed values (PAPM, 11.3 ± 1.3 liter/h; BP, 23.9 ± 3.0 liter/h). Predicted values for V_{SS} (PAPM, 12.1 liter; BP, 18.0 liter) also agreed well with the observed values (PAPM, 11.1 ± 2.3 liter; BP, 17.3 ± 4.9 liter). Predicted concentration in plasma-time profiles for humans approximated the observed profiles (Fig. 7).

Observed urinary recoveries of PAPM and BP in humans were 19.5 ± 8.0 and 97.9 ± 3.2%, respectively.

DISCUSSION

In the preclinical stage for developing new drugs, it is important to predict the pharmacokinetics in humans by using only animal data (13). In previous reports, a physiologically based pharmacokinetic model was successfully used to extrapolate animal data to humans (16). Animal scale-up using allometric interspecies scaling (3), however, may be more useful because of the simplicity of the experiments and of the analysis of data. Interspecies anatomic and physiological variations are correlated with BW or organ weight, which is known as allometry (1). This allometric technique has been developed by Dedrick (4) and extended by Boxenbaum (2) and others (14, 18). Recently, on the basis of allometric animal scale-up, the pharmacokinetics of some beta-lactam antibiotics has been successfully extrapolated from animals to humans (10).

In the present study, we examined the pharmacokinetics of PAPM-BP, a new carbapenem, in six animal species and predicted its pharmacokinetics in humans from animal data. We used allometric equations to predict CL_{tot} and V_{SS}. Then, we tried to predict two-phase plasma disposition kinetics of PAPM-BP by the complex Dedrick plot. In their paper on comparative methotrexate pharmacokinetics, De-

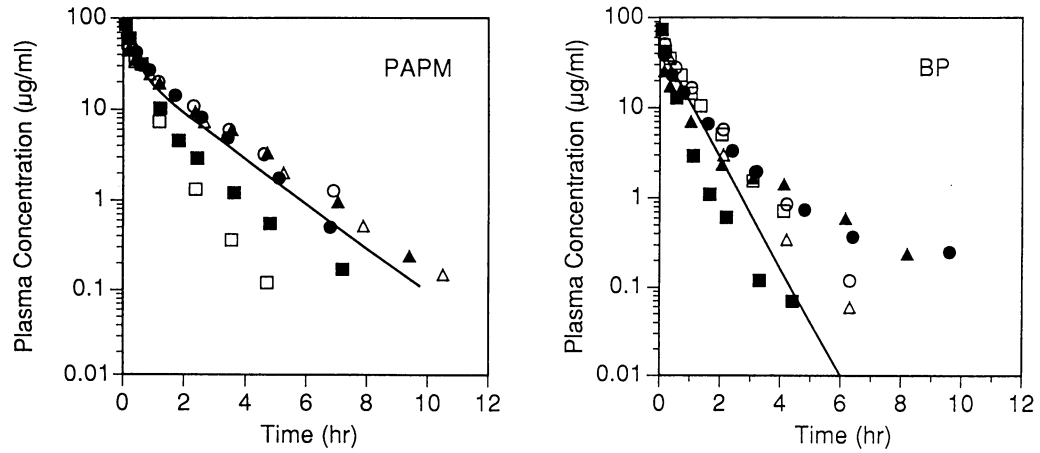

FIG. 6. Complex Dedrick plot of concentrations of PAPM and BP in plasma in mice (△), guinea pigs (▲), rats (□), rabbits (■), monkeys (○), and dogs (●). Each point represents the data in Fig. 2 replotted after normalizing concentration in plasma and time for humans. All points in each figure were fitted to the two-exponent equations indicated by solid lines.

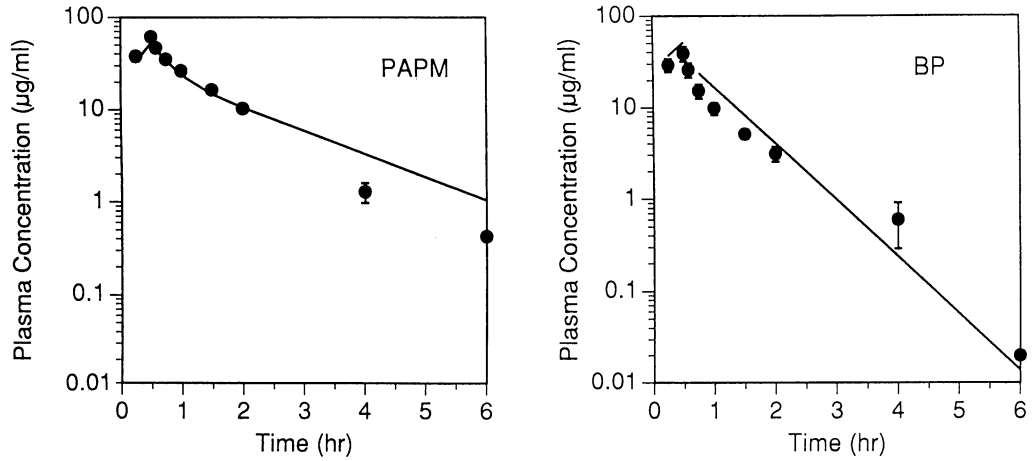

FIG. 7. Comparison of predicted and observed concentrations of PAPM and BP in human plasma after i.v. drip infusion of PAPM-BP (750/750 mg per body) for 30 min. Each point and vertical bar represents the mean ± standard deviation for five healthy male volunteers. Each line represents the values predicted by complex Dedrick plot. Predicted lines were obtained from the fitted lines in Fig. 6.

drick showed that biexponential concentration in plasma-time curves from every species studied were superimposable once concentrations in plasma were normalized for the dose administered and chronological times were normalized for the allometry of clearance (CL_{tot}) (4). This approach graphically demonstrated the basic similarities between species with regard to drug elimination processes. Boxenbaum has named this approach the Dedrick plot (1). It can be applied to drugs with no species difference for V_{SS} divided by BW, and he has explored its ramifications as the complex Dedrick plot. As with the Dedrick plot, superimposabilities of biexponential data from several species occur in the complex Dedrick plot provided that concentration in plasma and chronological times are normalized for the dose and for the allometry of CL_{tot} and the V_{SS}, as described in the prediction procedures above in Materials and Methods.

In extrapolating animal data to humans by the allometric technique, it is important to examine the linearity of the pharmacokinetics. As shown in Fig. 3, the pharmacokinetics of PAPM and BP are both linear. It is reported that the prediction is more successful when serum protein binding of a drug is considered in allometric scaling (12). Serum protein binding of PAPM in each animal species examined was less than 10%; therefore, CL_{tot} and V_{SS} of PAPM extrapolated well. On the other hand, serum protein binding of BP varied among the species, including humans. Considering the high level of urinary excretion, CL_{tot} of BP is mainly dominated by urinary excretion. CL_R of BP in each animal species exceeded the glomerular filtration rate and was close to renal plasma flow. Therefore, BP is extensively secreted from renal tubular cells, suggesting that the renal excretion of BP is independent of serum protein binding. In addition, the V_{SS} of BP in each species is relatively small and might be independent of the extent of serum protein binding. Taking these facts into account, we extrapolated CL_{tot} and V_{SS} of BP to humans without serum protein binding data and obtained good predictions.

In the studies of human pharmacokinetics, the BWs of human subjects varied minimally, which is normally not the case in the clinical situation. Therefore, in order to estimate the pharmacokinetics of PAPM-BP in patients whose BWs are far from 60 kg, actual BWs must be considered, as described in the prediction procedures.

In contrast to cilastatin, BP is not an inhibitor of renal dehydropeptidase-I (15). Cilastatin is combined with imipenem to lessen hydrolysis of imipenem by dehydropeptidase-I in the kidney (8). Therefore, urinary recoveries of PAPM after PAPM-BP administration are low compared with those of imipenem after imipenem-cilastatin administration in animals and humans (17). Clinical efficacies of PAPM-BP and imipenem-cilastatin, however, have been reported to be comparable for urinary tract infections. According to the Japanese Urinary Tract Infection Committee criteria, efficacy rates have been calculated to be 86.3 and 79.8% for PAPM-BP and imipenem-cilastatin, respectively, suggesting that urinary concentrations of PAPM are high enough to exert antimicrobial effects in spite of the low level of urinary recovery (9).

REFERENCES

1. **Boxenbaum, H.** 1982. Interspecies scaling, allometry, physiological time, and the ground plan of pharmacokinetics. J. Pharmacokinet. Biopharm. **10**:201–227.
2. **Boxenbaum, H.** 1984. Interspecies pharmacokinetic scaling and the evolutionary-comparative paradigm. Drug Metab. Rev. **15**: 1071–1121.
3. **Boxenbaum, H., and R. Ronfeld.** 1983. Interspecies pharmacokinetic scaling and the Dedrick plots. Am. J. Physiol. **245**:R768–R774.
4. **Dedrick, R. L.** 1973. Animal scale-up. J. Pharmacokinet. Biopharm. **1**:435–461.
5. **Hisaoka, M., M. Ichikawa, and T. Terao.** 1991. Microbiological assay method for the determination of panipenem concentrations in body fluids. Chemotherapy (Tokyo) **39**(Suppl. 3):190–196.
6. **Hisaoka, M., H. Naganuma, Y. Yamazaki, H. Takahagi, and Y. Kawahara.** 1991. High-performance liquid chromatography (HPLC) for the determination of panipenem/betamipron concentration in body fluids. Chemotherapy (Tokyo) **39**(Suppl. 3):197–205.
7. **Inoue, K., Y. Hamana, and S. Mitsuhashi.** 1991. Antibacterial activity of panipenem, a new carbapenem antibiotic. Chemotherapy (Tokyo) **39**(Suppl. 3):1–13.
8. **Kropp, H., J. G. Sundelof, R. Hajdu, and F. M. Kahan.** 1982. Metabolism of thienamycin and related carbapenem antibiotics by the renal dipeptidase, dehydropeptidase-I. Antimicrob. Agents Chemother. **22**:62–70.
9. **Kumazawa, J., and T. Matsumoto.** 1992. Phase III comparative

clinical trial of panipenem/betamipron with imipenem/cilastatin sodium for the treatment of complicated urinary tract infections. Nishinihon J. Urol. **54**:254–271.

10. **Matsushita, H., H. Suzuki, Y. Sugiyama, Y. Sawada, T. Iga, M. Hanano, and Y. Kawaguchi.** 1990. Prediction of the pharmacokinetics of cefodizime and cefotetan in humans from pharmacokinetic parameters in animals. J. Pharmacobio-Dyn. **13**:602–611.
11. **McGovren, J. P., M. G. Williams, and J. C. Stewart.** 1988. Interspecies comparision of acivicin pharmacokinetics. Drug Metab. Dispos. **16**:18–22.
12. **Mitsuhashi, Y., Y. Sugiyama, S. Ozawa, T. Nitanai, K. Sasahara, K. Nakamura, M. Tanaka, T. Nishimura, M. Inaba, and T. Kobayashi.** 1990. Prediction of ACNU plasma concentration-time profiles in humans by animal scale-up. Cancer Chemother. Pharmacol. **27**:20–26.
13. **Mordenti, J.** 1985. Forecasting cephalosporin and monobactam antibiotic half-lives in humans from data collected in laboratory animals. Antimicrob. Agents Chemother. **27**:887–891.
14. **Mordenti, J.** 1985. Man versus beast: pharmacokinetic scaling in mammals. J. Pharm. Sci. **75**:1028–1040.
15. **Naganuma, H., H. Tokiwa, Y. Hirouchi, Y. Kawahara, J. Fukushige, M. Fukami, K. Hirota, S. Muramatsu, H. Takahagi, K. Inui, Y. Tanigawara, M. Yasuhara, R. Hori, and S. Kuwahara.** 1991. Nephroprotective effect and its mechanism of betamipron. 1. Relation of renal transport. Chemotherapy (Tokyo) **39**(Suppl. 3):166–177.
16. **Nakashima, E., K. Yokogawa, F. Ichimura, K. Kurata, H. Kido, N. Yamaguchi, and T. Yamana.** 1987. A physiologically based pharmacokinetic model for biperiden in animals and its extrapolation to humans. Chem. Pharm. Bull. **35**:718–725.
17. **Norrby, S. R., K. Alestig, B. Bjornegard, L. A. Burman, F. Ferber, J. L. Huber, K. H. Jones, F. M. Kahan, J. S. Kahan, H. Kropp, M. A. P. Meisinger, and J. G. Sundelof.** 1983. Urinary recovery of *N*-formimidoyl thienamycin (MK0787) as affected by coadministration of *N*-formimidoyl thienamycin dehydropeptidase inhibitors. Antimicrob. Agents Chemother. **23**: 300–307.
18. **Rowland, M.** 1985. Physiological pharmacokinetic models and interanimal species scaling. Pharmacol. Ther. **29**:49–68.
19. **Swabb, E. A., and D. P. Bonner.** 1983. Prediction of aztreonam pharmacokinetics in humans based on data from animals. J. Pharmacokinet. Biopharm. **11**:215–223.
20. **Yamaoka, K., T. Nakagawa, and T. Uno.** 1978. Statistical moments in pharmacokinetics. J. Pharmacokinet. Biopharm. **6**:547–558.
21. **Yamaoka, K., Y. Tanigawara, T. Nakagawa, and T. Uno.** 1981. A pharmacokinetic analysis program (MULTI) for microcomputer. J. Pharmacobio-Dyn. **4**:879–885.